Ray and wave instabilities in twisted graded-index optical fibers

(Article begins on next page)

20 April 2024

Ray and wave instabilities in twisted graded-index optical fibers

S. Longhi, G. Della Valle, and D. Janner

Istituto Nazionale per la Fisica della Materia, Dipartimento di Fisica and IFN-CNR, Politecnico di Milano,
Piazza L. da Vinci 32, I-20133 Milan, Italy

We study ray and wave propagation in an elliptical graded-index optical fiber or lens with a twisted axis and show analytically the existence of an instability for both ray trajectories and beam moments in a finite range of axis twist rate embedded within the spatial frequencies of periodically focused rays for the untwisted fiber. By considering the paraxial ray equations and the paraxial wave dynamics in a rotating frame that follows the fiber axis twist, we reduce the dynamical problem of ray trajectories to the classical Blackburn's pendulum, which shows a dynamical instability, corresponding to classical diverging trajectories, due to the competing effects of confining potential, Coriolis force, and centrifugal force. A closed set of linear evolution equations for generalized beam moments are also derived from the paraxial wave equation in the rotating reference frame, revealing the existence of a dynamical moment instability in addition to the trajectory instability. A detailed analysis of beam propagation is presented in case of a Gaussian beam, and different dynamical regimes are discussed.

I. INTRODUCTION

The study of ray and wave propagation in confining optical structures, such as optical fibers, waveguides, photonic crystals, periodic focusing systems, and resonators plays a major role in the understanding the basic properties of light guiding underlying the operation of many optical and photonic components and laser devices. The close analogy of wave optics and wave mechanics, and their respective limits of geometric optics and Newtonian dynamics (see, e.g., Refs. [1,2]), has continuously brought into the optical research many ideas and concepts drawn from quantum physics, most notably the recent invention and development since the last two decades of photonic crystals (see, e.g., Ref. [3]). At the same time, guided optical systems may be used to test many quantum-mechanical effects including, among others, the issue of tunneling times across a potential barrier [4–7], quantum chaos [8], Bloch oscillations in a periodic potential [9–11], Anderson localization [12–14], and wave packet dynamics of atoms in high fields [15]. The most simple and studied analogy between guided optics and quantum mechanics is perhaps the parabolic graded-index (GRIN) fiber or lens and the quantum harmonic oscillator (see, e.g., Refs. [16–21]). This analogy is further attractive in the nonlinear propagation regime, i.e., when the optical Kerr effect is considered, since in this case beam propagation in the graded-index parabolic fiber bears a close connection with the dynamics of an attractive Bose-Einstein condensate in a harmonic potential. Such an analogy stems from the formal equivalence between the nonlinear Schrödinger equation of the optical field and the Gross-Pitaevskii equation for the macroscopic condensate wave function in the mean-field limit (see, e.g., Refs. [22,23]). A rather general and well-known phenomenon of ray and wave propagation in parabolic graded-index fibers (or in periodically focusing systems) is the appearance of ray and wave instabilities when the optical axis deviates from straightness [24–26] or in presence of perturbations or modulations, either periodic, quasi-periodic, or stochastic [13,22,26,27]. Such instabilities can be ultimately explained in terms of either a direct or a parametric forcing of the unforced harmonic oscillator dynamics, and may persist even in presence of nonlinear effects [22,28].

In this work we study analytically and numerically the dynamics of ray and wave propagation in an astigmatic parabolic-index optical fiber or lens with a twisted optical axis in the linear propagation regime. The geometric-optic limit of ray dynamics in the twisted fiber turns out to be equivalent to the dynamics of a classical Blackburn's pendulum (see, for instance, Ref. [29]), and shows a dynamical instability within a finite range of fiber twist rate, corresponding to classical diverging trajectories, due to the competing effects of confining potential, Coriolis force, and centrifugal force. Owing to the parabolic form of the fiber index profile, the motion of the beam center of mass is ruled out by the same geometric-optic ray equations and thus shows the same trajectory instability. A closed set of equations for generalized mean beam parameters (beam moments) is also derived, which show the occurrence of a beam moment instability in addition to the trajectory instability. Such an instability bears a close connection with the dynamic instability of a Bose-Einstein condensate subjected to a rotating harmonic potential [30,31], which has been studied in the hydrodynamic approximation (i.e., in the strongly nonlinear regime) of the nonlinear Schrödinger equation [30,31] and related to the spontaneous formation of vortices (see, for instance, Refs. [30,32,33]). The paper is organized as follows. In Sec. II the basic model of the graded-index astigmatic fiber with a linearly twisted axis is presented, and the basic beam propagation equation in the paraxial and scalar approximations is derived in a rotating reference frame. Section III deals with the geometric-optic limit and the classical Blackburn's pendulum analogy, revealing the existence of a trajectory instability for the optical rays. Section IV is devoted to the beam propagation problem. By using a beam moment method, we show analytically that in the dynamical

region corresponding to geometric-optic ray instability a beam moment instability occurs as well. Such an instability manifests itself in a growth of beam ellipticity and beam size even though the beam remains centered on the fiber axis. A detailed analysis is presented in case of Gaussian beam propagation. Finally in Sec. V the main conclusions are outlined.

II. RAY AND WAVE PROPAGATION IN AN ASTIGMATIC GRADED-INDEX OPTICAL FIBER WITH A TWISTED AXIS: BASIC EQUATIONS

We consider a graded-index optical fiber or GRIN lens with an astigmatic parabolic index profile of the form

$$n(X,Y) = n_0 - \tfrac{1}{2}(g_x X^2 + g_y Y^2), \tag{1}$$

where n_0 is the on-axis fiber refractive index, $g_x = 2n_0\Delta/r_{cx}^2$ and $g_y = 2n_0\Delta/r_{cy}^2$ are the graded-index parameters in the transverse X and Y directions, Δ ($\Delta \ll 1$) is the relative index difference between the core and the cladding, and r_{cx} and r_{cy} are the semiaxis sizes of the elliptical fiber core. We further assume that the fiber is twisted around its axis Z and indicate by $\theta = \theta(Z)$ the twist angle. If we account for the fiber twist, the refractive index profile of the fiber then reads

$$n(X,Y,Z) = n_0 - n_1(X,Y,Z), \tag{2}$$

where

$$n_1(X,Y,Z) = \tfrac{1}{2}[g_x(X\cos\theta + Y\sin\theta)^2 + g_y(-X\sin\theta + Y\cos\theta)^2]. \tag{3}$$

The ray dynamics in the paraxial approximation for the ray displacements $X(Z)$ and $Y(Z)$ is governed by the ray equations, as derived from Fermat's principle, which for $|n_1| \ll n_0$ read (see, for instance, Ref. [34])

$$\frac{d^2 X}{dZ^2} + \frac{1}{n_0}\frac{\partial n_1}{\partial X} = 0, \tag{4}$$

$$\frac{d^2 Y}{dZ^2} + \frac{1}{n_0}\frac{\partial n_1}{\partial Y} = 0. \tag{5}$$

Similarly, the wave dynamics, in the paraxial and scalar approximations and assuming that the beam width is sufficiently smaller as compared to r_{cx} and r_{cy}, is governed by the following equation for the wave field $\psi(X,Y,Z)$ (see, e.g., Refs. [35–37]):

$$i\frac{\partial\psi}{\partial Z} = -\frac{1}{2k}\nabla_\perp^2\psi + \frac{k}{n_0}n_1(X,Y,Z)\psi, \tag{6}$$

where $\nabla_\perp^2$ is the transverse Laplacian, $k = n_0\omega/c$ is the propagation constant in the cladding, and ω the angular frequency of the wave. For the following analysis, it is worth introducing the dimensionless spatial variables

$$z = \sqrt{\frac{g_x}{2n_0}}Z, \quad x' = \left(2k\sqrt{\frac{g_x}{2n_0}}\right)^{1/2}X, \quad y' = \left(2k\sqrt{\frac{g_x}{2n_0}}\right)^{1/2}Y \tag{7}$$

and the ellipticity fiber core parameter

$$\beta = \frac{g_y}{g_x} = \left(\frac{r_{cx}}{r_{cy}}\right)^2, \tag{8}$$

which we assume to be larger than one for the sake of definiteness. Using Eqs. (3), (7), and (8), the propagation wave equation (6) takes the scaled form

$$i\frac{\partial\psi}{\partial z} = [-\nabla_\perp^2 + V'(x',y',z)]\psi, \tag{9}$$

where

$$V'(x',y',z) = \tfrac{1}{2}(\sigma_{xx}x'^2 + \sigma_{yy}y'^2 + 2\sigma_{xy}x'y'), \tag{10}$$

$$\sigma_{xx}(z) = \cos^2\theta(z) + \beta\sin^2\theta(z), \tag{11}$$

$$\sigma_{yy}(z) = \sin^2\theta(z) + \beta\cos^2\theta(z), \tag{12}$$

$$\sigma_{xy}(z) = (1 - \beta)\sin\theta(z)\cos\theta(z), \tag{13}$$

and the Laplacian acts on the normalized transverse spatial variables x' and y'. Similarly, the ray equations (4) and (5) in the dimensionless spatial variables read

$$\frac{d^2 x'}{dz^2} = -2(\sigma_{xx}x' + \sigma_{xy}y'), \tag{14}$$

$$\frac{d^2 y'}{dz^2} = -2(\sigma_{xy}x' + \sigma_{yy}y'). \tag{15}$$

Instead of considering the ray or wave dynamics in the (x',y',z) reference frame, it is worth introducing a rotating reference frame (x,y,z) that follows the fiber twist, i.e., we make the change of variables (see Fig. 1)

$$x = x'\cos\theta(z) + y'\sin\theta(z), \tag{16}$$

$$y = -x'\sin\theta(z) + y'\cos\theta(z). \tag{17}$$

In the rotating reference frame, the scalar wave equation (9) takes the canonical form

$$i\frac{\partial\psi}{\partial z} = \mathcal{H}\psi, \tag{18}$$

where

$$\mathcal{H} \equiv -\left(\frac{\partial^2}{\partial x^2} + \frac{\partial^2}{\partial y^2}\right) + i\frac{d\theta}{dz}\left(x\frac{\partial}{\partial y} - y\frac{\partial}{\partial x}\right) + V(x,y) \tag{19}$$
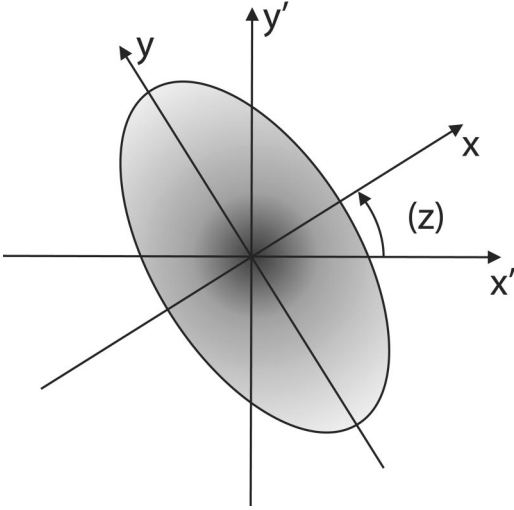
and

FIG. 1. Beam propagation in an astigmatic graded-index optical fiber. In the figure, (x',y') is the laboratory reference frame, (x,y) is the rotating reference frame that follows the fiber twist, $\theta(z)$ is the twist angle, and z is the fiber propagation axis.

$$V(x,y) = \frac{1}{2}(x^2 + \beta y^2). \qquad (20)$$

Similarly, in the rotating reference frame the ray equations (14) and (15) take the form

$$\frac{d^2x}{dz^2} = -\left[2 - \left(\frac{d\theta}{dz}\right)^2\right]x + 2\frac{d\theta}{dz}\frac{dy}{dz}, \qquad (21)$$

$$\frac{d^2y}{dz^2} = -\left[2\beta - \left(\frac{d\theta}{dz}\right)^2\right]y - 2\frac{d\theta}{dz}\frac{dx}{dz}. \qquad (22)$$

A particularly simple and important case is that of a constant twist rate, i.e., $d\theta/dz = \Phi = \text{const}$, which corresponds to a linear increase of the twist angle with propagation distance. Note that in this case the ray and wave dynamics in the rotating reference frame, as ruled by Eqs. (18)–(22), is governed by a set of autonomous equations. In the following, we will limit our analysis to the linear twist case.

III. RAY ANALYSIS

The ray equations (21) and (22) in the rotating reference frame can be written in the compact Newtonian form as

$$m\frac{d^2\mathbf{r}}{dz^2} = -\boldsymbol{\nabla} V + m\Omega^2\mathbf{r} - 2m\boldsymbol{\Omega} \times \frac{d\mathbf{r}}{dz}, \qquad (23)$$

where $\mathbf{r} = (x,y)$ is the ray displacement, $\boldsymbol{\Omega} = (d\theta/dz)\mathbf{u}_z = \Phi\mathbf{u}_z$, $V(x,y)$ is given by Eq. (20), and $m = 1/2$. In this form, Eq. (23) describes the Newtonian motion of a mass m in a noninertial reference frame, rotating at the angular frequency $\boldsymbol{\Omega}$, subjected to an anisotropic harmonic potential $V(x,y)$. Such an equation is discussed in many mechanics textbooks and, as shown by Lamb [29], it describes the dynamics of Blackburn's pendulum, a pendulum with different effective lengths in two orthogonal directions on a turntable. The

normal-mode frequencies λ of the pendulum can be easily found by looking for a solution of Eqs. (21) and (22) in the form:

$$\begin{pmatrix} x(z) \\ y(z) \end{pmatrix} = \begin{pmatrix} \bar{x} \\ \bar{y} \end{pmatrix} \exp(i\lambda z), \qquad (24)$$

which yields the following second-order determinantal equation for λ^2:

$$\lambda^4 - 2(1 + \beta + \Phi^2)\lambda^2 + (2 - \Phi^2)(2\beta - \Phi^2) = 0. \qquad (25)$$

In absence of rotation, i.e., for $\Phi = 0$, the normal-mode frequencies are given by $\lambda_x = \sqrt{2}$ and $\lambda_y = \sqrt{2\beta}$, i.e., are those of the uncoupled harmonic oscillation modes in the x and y directions. In presence of rotation, an inspection of Eq. (25) reveals that the frequency λ becomes imaginary, showing the appearance of an unbound motion, when the angular frequency Φ of rotation satisfies the condition

$$\sqrt{2} < \Phi < \sqrt{2\beta}. \qquad (26)$$

In terms of our fiber model, this means that the ray trajectories are unbounded, i.e., the fiber ceases to trap paraxial rays, when the fiber twist rate Φ falls in between the spatial frequencies λ_x and λ_y that define the periodic focusing properties along the x and y directions of the untwisted graded-index fiber, i.e., the GRIN fiber "pitch" in the two directions. Note that the range of ray instability shrinks as the ellipticity parameter β gets close to one, i.e., when the fiber becomes circular. From a physical viewpoint, the appearance of the instability as the twist rate Φ increases above λ_x is due to the increase of the centrifugal force in Eq. (23), which becomes larger than the attractive harmonic force in the x direction. However, as Φ is increased above λ_y, though the centrifugal force increases, the Coriolis force becomes important to restore the confinement, and paraxial rays are thus again trapped by the graded-index fiber.

IV. WAVE ANALYSIS

In this section we study in detail the beam propagation dynamics in the twisted optical fiber using the beam propagation equation (18) written in the rotating reference frame. We will first show that the dynamical equations for the beam center of mass are the same as those obtained in the geometric-optic limit. Further insights into the dynamics of an arbitrary beam propagating into the twisted fiber are then given by deriving a closed system of coupled linear equations for certain average beam parameters, or beam moments. Such an analysis reveals the existence of a beam moment instability in addition to the ray (or beam center) instability. A detailed analysis is finally presented for the dynamics of Gaussian beams, which propagate along the fiber maintaining their invariant functional form. For the following analysis and considering the mechanical analogy outlined in the preceding section, it is worth observing that Eq. (18) is the quantum-mechanical Schrödinger equation of the classical Blackburn's pendulum, with $m = 1/2$ and $\hbar = 1$. Note that, since the equation is written in a noninertial reference frame, the Hamiltonian $\mathcal{H}$, given by Eq. (19), contains the

additional angular momentum operator $\mathcal{L}_z = -i(x\partial/\partial y - y\partial/\partial x)$ (see, for instance, Ref. [38]). In a different but similar interpretation, Eq. (18) can be viewed as a Schrödinger equation of a charged particle in an inertial reference frame subjected to an anisotropic harmonic force in presence of a static magnetic field oriented along the fiber z axis [38]. Since the Hamiltonian $\mathcal{H}$ given by Eq. (19) is self-adjoint, for any z-independent operator $\mathcal{A}$, the mean value $\langle\mathcal{A}\rangle \equiv \int dxdy\, \psi^* \mathcal{A}\psi$ satisfies the evolution equation

$$\frac{d\langle\mathcal{A}\rangle}{dz} = -i\langle[\mathcal{A},\mathcal{H}]\rangle, \tag{27}$$

which involves the commutator $[\mathcal{A},\mathcal{H}] = \mathcal{A}\mathcal{H} - \mathcal{H}\mathcal{A}$. Equation (27) will be used to study the dynamics of certain mean beam parameters. Without loss of generality, we will assume in the following the normalization condition $\int dxdy\,|\psi|^2 = 1$ for the optical field.

A. Beam trajectory analysis

Let us first consider the evolution equations for the beam center of mass coordinates:

$$\langle x\rangle = \int dxdy\, x|\psi|^2, \quad \langle y\rangle = \int dxdy\, y|\psi|^2. \tag{28}$$

Using the commutation rules

$$[x,\mathcal{H}] = 2\frac{\partial}{\partial x} + i\Phi y, \tag{29}$$

$$[y,\mathcal{H}] = 2\frac{\partial}{\partial y} - i\Phi x, \tag{30}$$

$$\left[\frac{\partial}{\partial x},\mathcal{H}\right] = \frac{\partial V}{\partial x} + i\Phi\frac{\partial}{\partial y} = x + i\Phi\frac{\partial}{\partial y}, \tag{31}$$

$$\left[\frac{\partial}{\partial y},\mathcal{H}\right] = \frac{\partial V}{\partial y} - i\Phi\frac{\partial}{\partial x} = \beta y - i\Phi\frac{\partial}{\partial x} \tag{32}$$

from Eq. (27) we obtain the following set of coupled equations:

$$\frac{d\langle x\rangle}{dz} = -2i\left\langle\frac{\partial}{\partial x}\right\rangle + \Phi\langle y\rangle, \tag{33}$$

$$\frac{d\langle y\rangle}{dz} = -2i\left\langle\frac{\partial}{\partial y}\right\rangle - \Phi\langle x\rangle, \tag{34}$$

$$\frac{d}{dz}\left\langle\frac{\partial}{\partial x}\right\rangle = -i\langle x\rangle + \Phi\left\langle\frac{\partial}{\partial y}\right\rangle, \tag{35}$$

$$\frac{d}{dz}\left\langle\frac{\partial}{\partial y}\right\rangle = -i\beta\langle y\rangle - \Phi\left\langle\frac{\partial}{\partial x}\right\rangle. \tag{36}$$

If we eliminate from these equations the mean values $\langle\partial/\partial x\rangle$ and $\langle\partial/\partial y\rangle$, one easily obtains for $\langle x\rangle$ and $\langle y\rangle$ the same

coupled equations (21) and (22) valid in the geometric-optic limit, i.e., the beam trajectory coincides with the ray trajectory. This result, which follows from the quadratic dependence of the refractive index profile on x and y, demonstrates that a beam trajectory instability occurs, as in the geometric-optic limit, when the twist rate satisfies the condition expressed by Eq. (26).

B. Beam moment analysis

To better characterize the beam propagation properties, it is worth considering the dynamics of some mean beam parameters related to, e.g., the beam spot sizes along the two transverse x and y directions, beam angular momentum, and higher-order beam moments. Beam moment analysis has been widely used to study exact (or approximate) beam propagation in nonastigmatic optical systems, either in the linear or nonlinear propagation regimes [22,23,39]. In a circular graded-index fiber, a set of closed equations for few beam moments (usually three) can be derived (see, e.g., Ref. [22]). The introduction of a fiber twist, associated with the astigmatic refractive index profile, leads to a coupling of beam moments in the orthogonal x and y directions, so that to obtain a set of closed equations one needs to include in the calculations up to ten beam moments, namely $\langle x^2\rangle$, $\langle y^2\rangle$, $\langle x(\partial/\partial x)\rangle$, $\langle y(\partial/\partial y)\rangle$, $\langle\partial^2/\partial x^2\rangle$, $\langle\partial^2/\partial y^2\rangle$, $\langle x(\partial/\partial y)\rangle$, $\langle y(\partial/\partial x)\rangle$, $\langle\partial^2/\partial x\partial y\rangle$, and $\langle xy\rangle$. Indeed, using Eq. (27) one can show that (see Appendix A)

$$\frac{d}{dz}\langle x^2\rangle = -2i\left(1 + 2\left\langle x\frac{\partial}{\partial x}\right\rangle\right) + 2\Phi\langle xy\rangle, \tag{37}$$

$$\frac{d}{dz}\langle y^2\rangle = -2i\left(1 + 2\left\langle y\frac{\partial}{\partial y}\right\rangle\right) - 2\Phi\langle xy\rangle, \tag{38}$$

$$\frac{d}{dz}\left\langle x\frac{\partial}{\partial x}\right\rangle = -2i\left\langle\frac{\partial^2}{\partial x^2}\right\rangle - i\langle x^2\rangle + \Phi\left(\left\langle x\frac{\partial}{\partial y}\right\rangle + \left\langle y\frac{\partial}{\partial x}\right\rangle\right), \tag{39}$$

$$\frac{d}{dz}\left\langle y\frac{\partial}{\partial y}\right\rangle = -2i\left\langle\frac{\partial^2}{\partial y^2}\right\rangle - i\beta\langle y^2\rangle - \Phi\left(\left\langle x\frac{\partial}{\partial y}\right\rangle + \left\langle y\frac{\partial}{\partial x}\right\rangle\right), \tag{40}$$

$$\frac{d}{dz}\left\langle\frac{\partial^2}{\partial x^2}\right\rangle = -i - 2i\left\langle x\frac{\partial}{\partial x}\right\rangle + 2\Phi\left\langle\frac{\partial^2}{\partial x\partial y}\right\rangle, \tag{41}$$

$$\frac{d}{dz}\left\langle\frac{\partial^2}{\partial y^2}\right\rangle = -i\beta - 2i\beta\left\langle y\frac{\partial}{\partial y}\right\rangle - 2\Phi\left\langle\frac{\partial^2}{\partial x\partial y}\right\rangle, \tag{42}$$

$$\frac{d}{dz}\left\langle x\frac{\partial}{\partial y}\right\rangle = -i\beta\langle xy\rangle - 2i\left\langle\frac{\partial^2}{\partial x\partial y}\right\rangle + \Phi\left(\left\langle y\frac{\partial}{\partial y}\right\rangle - \left\langle x\frac{\partial}{\partial x}\right\rangle\right), \tag{43}$$
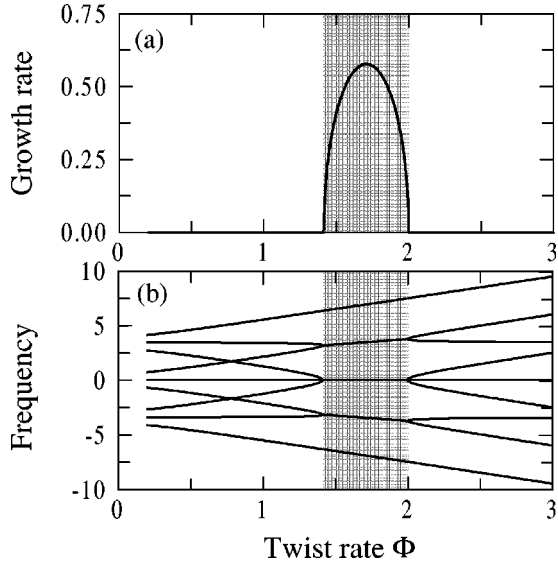
FIG. 2. (a) Real part (growth rate) of the most unstable eigenvalue of the moment matrix $\mathcal{M}$ vs fiber twist rate Φ and (b) imaginary parts (frequencies) of the matrix eigenvalues. Fiber ellipticity parameter $\beta=2$. The shaded areas correspond to the ray trajectory instability domain $\sqrt{2}<\Phi<\sqrt{2\beta}$.

$$\frac{d}{dz}\left\langle y\frac{\partial}{\partial x}\right\rangle = -i\langle xy\rangle - 2i\left\langle\frac{\partial^2}{\partial x\,\partial y}\right\rangle$$
$$+ \Phi\left(\left\langle y\frac{\partial}{\partial y}\right\rangle - \left\langle x\frac{\partial}{\partial x}\right\rangle\right), \quad (44)$$

$$\frac{d}{dz}\left\langle\frac{\partial^2}{\partial x\,\partial y}\right\rangle = -i\left\langle x\frac{\partial}{\partial y}\right\rangle - i\beta\left\langle y\frac{\partial}{\partial x}\right\rangle$$
$$+ \Phi\left(\left\langle\frac{\partial^2}{\partial y^2}\right\rangle - \left\langle\frac{\partial^2}{\partial x^2}\right\rangle\right), \quad (45)$$

$$\frac{d}{dz}\langle xy\rangle = -2i\left\langle x\frac{\partial}{\partial y}\right\rangle - 2i\left\langle y\frac{\partial}{\partial x}\right\rangle + \Phi(\langle y^2\rangle - \langle x^2\rangle).$$
$$(46)$$

The previous equations represent a system of nonhomogeneous linear equations. The eigenvalues of the 10×10 matrix $\mathcal{M}$ of the associated linear homogeneous system, whose elements depend on the fiber twist rate Φ and ellipticity parameter β, govern the beam moment stability. For parameter values where the matrix eigenvalues are purely imaginary, the imaginary parts of the eigenvalues provide the normal-mode oscillation frequencies of the beam moments. When the real part of at least one eigenvalue becomes positive, a beam moment instability appears. An analysis of the matrix eigenvalues, whose explicit expression is given in Appendix B, shows that eigenvalues with a positive real part exist in the parameter range where the ray trajectory instability occurs, i.e., when $\sqrt{2}<\Phi\sqrt{2\beta}$ [see Eq. (26)]. As an example, Fig. 2 shows the behavior of the real and imaginary parts of the matrix eigenvalues as functions of the fiber twist rate Φ for an ellipticity parameter $\beta=2$. From a physical point of

view, the existence of a beam moment instability means the divergence of mean beam parameters in addition to beam trajectory, in particular, of the beam transverse sizes. In fact, let us assume for the sake of clearness that the injected beam has its center of mass on the z axis, i.e., $\langle x\rangle=\langle y\rangle=0$, so that in absence of perturbations the beam center remains on the fiber axis during propagation. In this case, though the beam remains centered into the fiber axis, its transverse sizes along the x and y directions, given by $w_x=[\langle(x-\langle x\rangle)^2\rangle]^{1/2}=\langle x^2\rangle^{1/2}$ and $w_y=\langle y^2\rangle^{1/2}$, asymptotically grow. This behavior will be illustrated in detail in the following section in case of a Gaussian beam.

C. Gaussian beam dynamics

A particular and important case, which also helps us to clarify the onset of beam moment instability discussed in the preceding section is that of Gaussian beams, which propagate in the fiber without changing its functional form. In fact, let us search for a solution to the beam propagation equation (18) in the form of an astigmatic Gaussian beam:

$$\psi(x,y,z) = A(z)\exp\{-\gamma_x(z)[x-x_0(z)]^2 - \gamma_y(z)[y-y_0(z)]^2$$
$$- 2\rho(z)[x-x_0(z)][y-y_0(z)]\}, \quad (47)$$

where A is the complex-valued amplitude of the Gaussian beam, x_0 and y_0 are the real-valued beam center of mass coordinates, and γ_x, γ_y, ρ are the complex-valued parameters of the astigmatic Gaussian beam which determine beam sizes, beam phase front curvatures, and beam rotation angle. The conditions $\text{Re}(\gamma_x)>0$, $\text{Re}(\gamma_y)>0$, and $\text{Re}(\gamma_x)\text{Re}(\gamma_y)>[\text{Re}(\rho)]^2$ are assumed to ensure that $\int dxdy\,|\psi|^2<\infty$. Substitution of Eq. (47) into Eq. (18) yields a set of ordinary differential equations for the beam parameters. In particular, according to the general result of Sec. IV A, it is found that the beam center of mass coordinates $x_0(z)$ and $y_0(z)$ satisfy the ray trajectory equations (21) and (22), whereas the complex beam parameters γ_x, γ_y, and ρ satisfy the following coupled nonlinear equations:

$$\frac{d\gamma_x}{dz} = -4i\gamma_x^2 - 4i\rho^2 + \frac{i}{2} + 2\Phi\rho, \quad (48)$$

$$\frac{d\gamma_y}{dz} = -4i\gamma_y^2 - 4i\rho^2 + \frac{i\beta}{2} + 2\Phi\rho, \quad (49)$$

$$\frac{d\rho}{dz} = -4i\gamma_x\rho - 4i\gamma_y\rho + \Phi(\gamma_y - \gamma_x). \quad (50)$$

Finally, the complex beam amplitude $A(z)$ is then found by the equation

$$A(z) = A(0)\exp\left[-2i\int_0^z dz'\,\gamma_x(z') - 2i\int_0^z dz'\,\gamma_y(z')\right.$$
$$\left. - \frac{i}{2}\int_0^z dz'\,x_0^2(z') - \frac{i\beta}{2}\int_0^z dz'\,y_0^2(z')\right]. \quad (51)$$

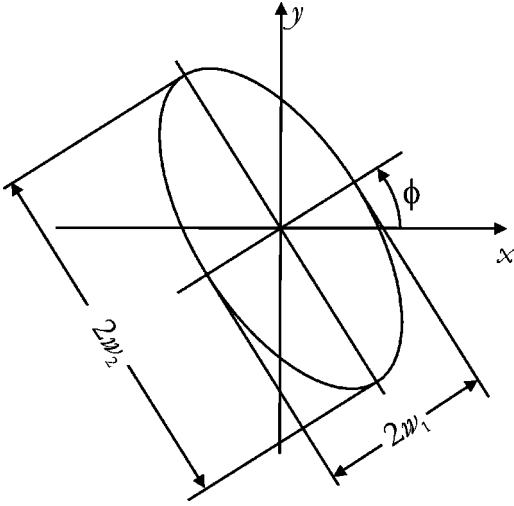Note that the dynamics of the beam parameters γ_x, γ_y, and ρ

FIG. 3. Astigmatic Gaussian beam profile, in the rotating reference frame (x,y), expressed by Eq. (47) with $x_0=y_0=0$. The relations between ellipse parameters w_1, w_2, ϕ, and complex beam parameters γ_x, γ_y, and ρ entering in Eq. (47) are given in the text [Eqs. (52)–(55)].

is decoupled from that of the beam center of mass coordinates $x_0(z)$, $y_0(z)$, so that we will consider the case of a Gaussian beam centered on the fiber axis $(x_0=y_0=0)$. In this case, one can easily show that the loci of points satisfying the condition $|\psi(x,y,z)/\psi(0,0,z)|^2=1/e^2$ is an ellipse of Cartesian equation $\mathrm{Re}(\gamma_x)x^2+\mathrm{Re}(\gamma_y)y^2+2\mathrm{Re}(\rho)xy=1$, whose semiaxes of length $w_1(z)$ and $w_2(z)$ are tilted with respect to the x axis by an angle $\phi(z)$, given by (see Fig. 3)

$$\tan(2\phi)=\frac{2\mathrm{Re}(\rho)}{\mathrm{Re}(\gamma_x)-\mathrm{Re}(\gamma_y)}. \tag{52}$$

The ellipticity parameter $\epsilon=(w_2/w_1)^2$ and semiaxes w_1 and w_2 are then given by

$$\epsilon=\frac{q+1}{q-1}, \tag{53}$$

$$w_2=\sqrt{\frac{\epsilon+1}{\mathrm{Re}(\gamma_x+\gamma_y)}}, \tag{54}$$

$$w_1=\frac{w_2}{\sqrt{\epsilon}}, \tag{55}$$

where $q=\mathrm{Re}(\gamma_x+\gamma_y)\sin(2\phi)/[2\mathrm{Re}(\rho)]$. We can first look for steady-state solutions to Eqs. (48)–(50), which correspond to Gaussian-like beams that follow the fiber twist, i.e., which are stationary in the rotating reference frame (x,y). In steady-state the beam parameter ρ is found to satisfy the algebraic cubic equation

$$c_0\rho^3+c_1\rho^2+c_2\rho+c_3=0, \tag{56}$$

where the coefficients c_1, c_2, and c_3 are given by

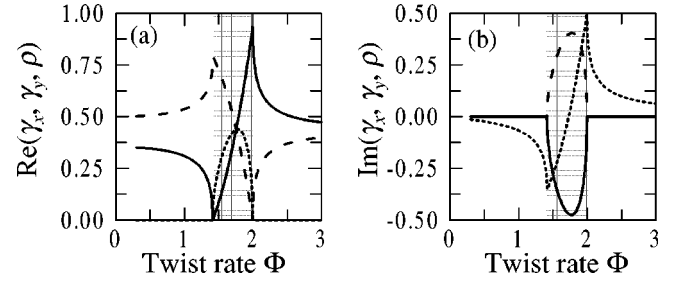$$c_0=32i\Phi(1-\beta)+64i\Phi(\beta-1), \tag{57}$$

FIG. 4. Steady-state Gaussian modes of the twisted fiber in the rotating reference frame. (a) and (b) show the real and imaginary parts, respectively, of the Gaussian beam parameters γ_x (solid lines), γ_y (dashed lines), and ρ (dotted lines) vs the fiber twist rate Φ. The shaded area represents the instability domain $\sqrt{2}<\Phi<\sqrt{2\beta}$, where the plotted solution does not lead to a confined Gaussian mode. Fiber ellipticity parameter $\beta=2$.

$$c_1=4(1+\beta-2\Phi^2)^2-16\beta, \tag{58}$$

$$c_2=-2i\Phi(1-\beta)(1+\beta-2\Phi^2), \tag{59}$$

$$c_3=-\frac{\Phi^2}{4}(1-\beta)^2. \tag{60}$$

The parameters γ_x and γ_y are then given by

$$\gamma_x=\sqrt{\frac{-8i\rho^2+i+4\Phi\rho}{8i}}, \tag{61}$$

$$\gamma_y=\sqrt{\frac{-8i\rho^2+i\beta-4\Phi\rho}{8i}}. \tag{62}$$

The solutions to Eqs. (56), (61), and (62) which are physically acceptable must satisfy the conditions $\mathrm{Re}(\gamma_x)>0$, $\mathrm{Re}(\gamma_y)>0$, and $\mathrm{Re}(\gamma_x)\mathrm{Re}(\gamma_y)>[\mathrm{Re}(\rho)]^2$. A numerical analysis of Eqs. (56), (61), and (62) shows that for a twist rate outside the domain of ray instability, i.e., for $\Phi<\sqrt{2}$ or $\Phi>\sqrt{2\beta}$, there exists one acceptable branch solution with γ_x, γ_y purely real and ρ purely imaginary (see Fig. 4). As Φ approaches the boundary of instabilities, either γ_x or γ_y goes to zero, indicating that the stationary modes degenerate into a strongly elliptical Gaussian beam. In the domain of ray instability, i.e., for $\sqrt{2}<\Phi\sqrt{2\beta}$, there exist two distinct solutions to Eqs. (56), (61), and (62), with complex values for γ_x, γ_y, ρ and with $\mathrm{Re}(\gamma_{x,y})>0$. One of such branch is shown in Fig. 4 inside the shaded area. However, since for both branches it turns out that $\mathrm{Re}(\gamma_x)\mathrm{Re}(\gamma_y)=[\mathrm{Re}(\rho)]^2$, these solutions do not correspond to localized Gaussian modes. In summary, the domain of ray and wave instability corresponds to that of nonexistence of stationary Gaussian modes in the rotating reference frame.

To get further physical insights into the dynamics of Gaussian beams, we integrated numerically Eqs. (48)–(50) using an accurate fourth-order Runge-Kutta algorithm with variable step; as an initial condition, we chose the astigmatic fundamental Gaussian mode of the untwisted fiber, which would propagate without distortion, i.e., we set $\gamma_x(0)$
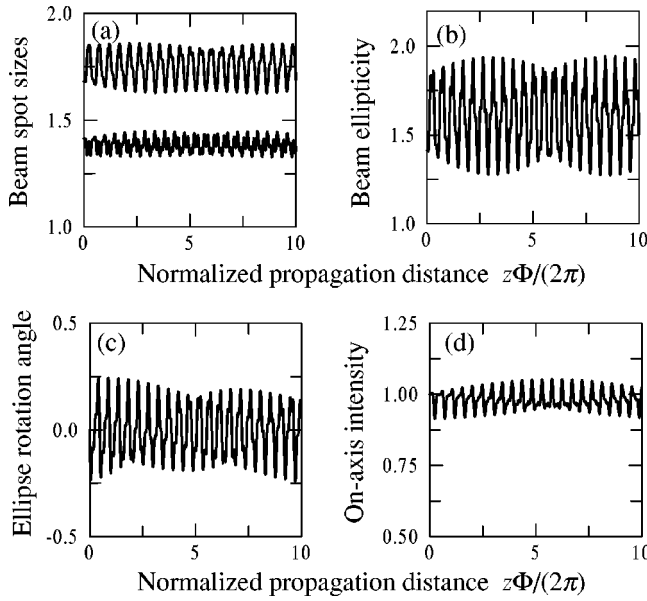
FIG. 5. Gaussian beam dynamics in the adiabatic propagation regime. (a) Behavior of elliptical Gaussian beam sizes w_1 and w_2 vs normalized propagation distance $n = z\Phi/(2\pi)$. (b) Behavior of beam ellipticity $\epsilon = (w_2/w_1)^2$ vs normalized propagation distance. (c) Behavior of beam ellipse rotation angle ϕ vs n. (d) Behavior of on-axis beam intensity $|A(z)|^2$, normalized to its value at $z=0$, vs n. The Gaussian beam parameters w_1, w_2, and ϕ are defined according to Fig. 3. The normalized variable n measures the propagation distance along the fiber in units of fiber rotational twist. Parameter values are $\beta=2$ and $\Phi=0.8$.

$=1/(2\sqrt{2})$, $\gamma_y(0)=\sqrt{\beta}/(2\sqrt{2})$, and $\rho(0)=0$. Three typical dynamical regimes have been found from the numerical analysis depending on the value of the twist rate Φ: the "adiabatic" regime for $\Phi<\sqrt{2}$, the instability regime for $\sqrt{2}<\Phi<\sqrt{2\beta}$, and the "averaging" regime for $\Phi>\sqrt{2\beta}$. Figures 5–7 show a typical evolution of Gaussian beam sizes $w_1(z)$, $w_2(z)$, beam amplitude $A(z)$, beam ellipticity $\epsilon(z)$, and tilting angle $\phi(z)$ (with respect to the rotating axis x; see Fig. 3) for a twist rate Φ chosen in the three above mentioned regimes. Note that, for a twist rate Φ below $\sqrt{2}$ (the adiabatic regime), small quasiperiodic variations of beam parameters are observed (see Fig. 5); in particular the angle ϕ displays small oscillations around zero [see Fig. 5(c)], indicating that the elliptical beam adiabatically follows the fiber twist. Conversely, inside the instability region (see Fig. 6) an exponential growth of beam ellipticity and beam size is observed [see Figs. 6(a) and 6(b)], with a corresponding decrease of the on-axis Gaussian beam amplitude [see Fig. 6(d)]. Note that the angle of elliptical beam stabilizes now to a nonvanishing zero value, i.e., the orientation of the elliptical beam in the rotating reference frame settles down to a stationary value and the beam then follows the fiber twist. However the fiber loses in this case its guiding properties. For a twist rate above $\sqrt{2\beta}$ (the averaging regime; see Fig. 7), a scenario similar to $\Phi<\sqrt{2}$ is observed, however here the angle $\phi(z)$ does not settle down to a steady-state value but varies almost linearly with longitudinal distance, i.e., the elliptical Gaussian beam orientation does not follow anymore the fiber twist.
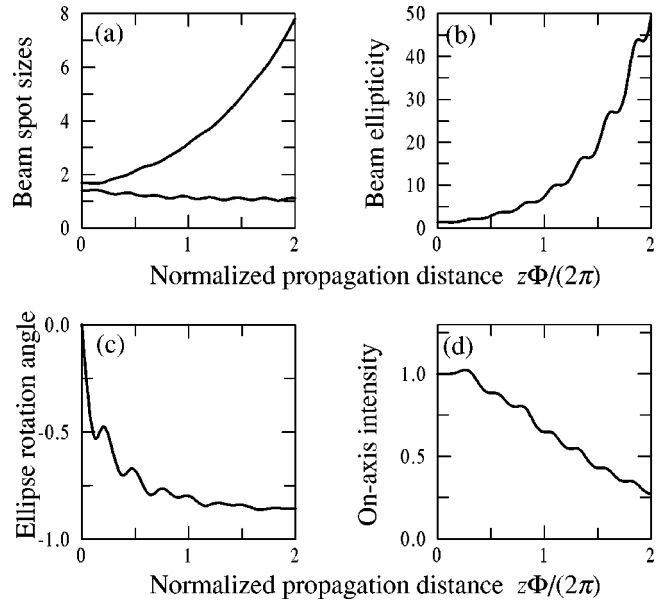

FIG. 6. Same as Fig. 5, but in the instability propagation regime. Parameter values are $\beta=2$ and $\Phi=1.8$.

Indeed, for very large twist rates, the beam dynamics is not able to follow the rapidly varying twist rate, and at leading order the beam sees an "average" graded-index fiber with a z-independent refractive index profile given by the spatial average, with respect to z, of the actual profile $n(x,y,z)$ given by Eqs. (2) and (3). This averaging leads to an average circular refractive index profile, and beam propagation is thus ruled out by the equations of a nonastigmatic parabolic graded-index fiber (for the concept of average guiding see, for instance, Ref. [15]).
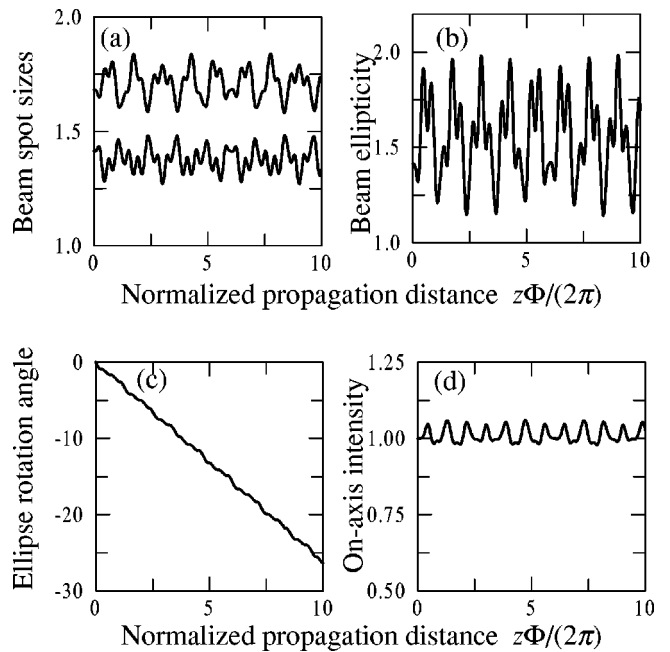

FIG. 7. Same as Fig. 5, but in the average propagation regime. Parameter values are $\beta=2$ and $\Phi=3$.

V. CONCLUSIONS

In this work we have studied analytically and numerically the ray and wave dynamics of an elliptical graded-index optical fiber with a twisted axis, and we have shown the existence of both a ray and a beam instability. The ray trajectories, found from Fermat's principle, turn out to be analogous to the trajectories of a rotating Blackburn's pendulum, the twist rate playing the same role as the rotational frequency (Sec. III). The existence of the twist-induced instability is due to the destabilizing effect of the centrifugal force as the rotation frequency increases above the lower oscillation frequency of the pendulum. However, as the rotation frequency becomes larger than the upper oscillation frequency of the pendulum, the stability of trajectories is restored due to the stabilizing effect of the Coriolis force. The beam propagation equation, in the scalar and paraxial approximation, is governed by a Schrödinger-like equation which is the quantum-mechanical model of the Blackburn's pendulum. For a constant twist rate, the dynamics can be made autonomous using a noninertial rotating reference frame (Sec. II). Due to the quadratic form of the refractive index profile, the beam trajectory coincides with that of optical rays in the geometric-optic limit, and thus any beam suffers from a trajectory instability (Sec. IV A). In addition, by means of a generalized beam moment analysis, we have shown that in the trajectory instability region a beam moment instability also occurs (Sec. IV B). A detailed analysis of the beam dynamics has been provided in case of Gaussian beam propagation (Sec. IV C). In particular, we have pointed out the existence of basically three distinct dynamical regimes: the adiabatic regime for low values of the twist rate, the instability regime for intermediate values of twist rate, and the averaging regime for high values of the twist rate. We envisage that our analysis may provide an experimentally accessible system in the optical field to study basic classical and quantum dynamical behaviors found in other physical systems, in particular, the center-of-mass instability of Bose-Einstein condensates in an anisotropic rotating trap [31,40].

APPENDIX A: DERIVATION OF THE BEAM MOMENT EQUATIONS

The set of closed equations for the beam moments given by Eqs. (37)–(46) in the text are the evolution equations of mean values for the operators x^2, y^2, $x(\partial/\partial x)$, $y(\partial/\partial y)$, $\partial^2/\partial x^2$, $\partial^2/\partial y^2$, $x(\partial/\partial y)$, $y(\partial/\partial x)$, $\partial^2/\partial x\partial y$, and xy. Such equations are easily obtained from Eq. (27) once the following commutation rules are used:

$$[x^2, \mathcal{H}] = 2 + 4x\frac{\partial}{\partial x} + 2i\Phi xy, \tag{A1}$$

$$[y^2, \mathcal{H}] = 2 + 4y\frac{\partial}{\partial y} - 2i\Phi xy, \tag{A2}$$

$$\left[x\frac{\partial}{\partial x}, \mathcal{H}\right] = x\frac{\partial V}{\partial x} + 2\frac{\partial^2}{\partial x^2} + i\Phi\left(x\frac{\partial}{\partial y} + y\frac{\partial}{\partial x}\right)$$
$$= x^2 + 2\frac{\partial^2}{\partial x^2} + i\Phi\left(x\frac{\partial}{\partial y} + y\frac{\partial}{\partial x}\right), \tag{A3}$$

$$\left[y\frac{\partial}{\partial y}, \mathcal{H}\right] = y\frac{\partial V}{\partial y} + 2\frac{\partial^2}{\partial y^2} - i\Phi\left(x\frac{\partial}{\partial y} + y\frac{\partial}{\partial x}\right)$$
$$= \beta y^2 + 2\frac{\partial^2}{\partial y^2} - i\Phi\left(x\frac{\partial}{\partial y} + y\frac{\partial}{\partial x}\right), \tag{A4}$$

$$\left[\frac{\partial^2}{\partial x^2}, \mathcal{H}\right] = \frac{\partial^2 V}{\partial x^2} + 2\frac{\partial V}{\partial x}\frac{\partial}{\partial x} + 2i\Phi\frac{\partial^2}{\partial x\partial y}$$
$$= 1 + 2x\frac{\partial}{\partial x} + 2i\Phi\frac{\partial^2}{\partial x\partial y}, \tag{A5}$$

$$\left[\frac{\partial^2}{\partial y^2}, \mathcal{H}\right] = \frac{\partial^2 V}{\partial y^2} + 2\frac{\partial V}{\partial y}\frac{\partial}{\partial y} - 2i\Phi\frac{\partial^2}{\partial x\partial y}$$
$$= \beta + 2\beta y\frac{\partial}{\partial y} - 2i\Phi\frac{\partial^2}{\partial x\partial y}, \tag{A6}$$

$$\left[x\frac{\partial}{\partial y}, \mathcal{H}\right] = x\frac{\partial V}{\partial y} + 2\frac{\partial^2}{\partial x\partial y} + i\Phi\left(y\frac{\partial}{\partial y} - x\frac{\partial}{\partial x}\right)$$
$$= \beta xy + 2\frac{\partial^2}{\partial x\partial y} + i\Phi\left(y\frac{\partial}{\partial y} - x\frac{\partial}{\partial x}\right), \tag{A7}$$

$$\left[y\frac{\partial}{\partial x}, \mathcal{H}\right] = y\frac{\partial V}{\partial x} + 2\frac{\partial^2}{\partial x\partial x} + i\Phi\left(y\frac{\partial}{\partial y} - x\frac{\partial}{\partial x}\right)$$
$$= xy + 2\frac{\partial^2}{\partial x\partial y} + i\Phi\left(y\frac{\partial}{\partial y} - x\frac{\partial}{\partial x}\right), \tag{A8}$$

$$\left[\frac{\partial^2}{\partial x\partial y}, \mathcal{H}\right] = \frac{\partial^2 V}{\partial x\partial y} + \frac{\partial V}{\partial x}\frac{\partial}{\partial y} + \frac{\partial V}{\partial y}\frac{\partial}{\partial x} + i\Phi\left(\frac{\partial^2}{\partial y^2} - \frac{\partial^2}{\partial x^2}\right)$$
$$= x\frac{\partial}{\partial y} + \beta y\frac{\partial}{\partial x} + i\Phi\left(\frac{\partial^2}{\partial y^2} - \frac{\partial^2}{\partial x^2}\right), \tag{A9}$$

$$[xy, \mathcal{H}] = 2y\frac{\partial}{\partial x} + 2x\frac{\partial}{\partial y} + i\Phi(y^2 - x^2), \tag{A10}$$

where the potential $V(x, y)$ is expressed by Eq. (20) given in the text.

APPENDIX B: BEAM MOMENT STABILITY—MATRIX EIGENVALUES

The eigenvalues λ of the 10×10 matrix $\mathcal{M}$ associated with the linear part of Eqs. (37)–(46) given in the text can be calculated analytically and read explicitly:

$$\lambda_{1,2} = 0, \tag{B1}$$

$$\lambda_{3,4} = \pm \sqrt{-1 - \beta - \Phi^2 - (1 - 2\beta + \beta^2 + 4\Phi^2 + 4\beta\Phi^2)^{1/2}}, \tag{B2}$$

$$\lambda_{5,6} = \pm \sqrt{-1 - \beta - \Phi^2 + (1 - 2\beta + \beta^2 + 4\Phi^2 + 4\beta\Phi^2)^{1/2}}, \tag{B3}$$

$$\lambda_{7,8} = \pm \sqrt{2} \sqrt{-1 - \beta - \Phi^2 - [(\Phi^2 - 2\beta)(\Phi^2 - 2)]^{1/2}}, \tag{B4}$$

$$\lambda_{9,10} = \pm \sqrt{2} \sqrt{-1 - \beta - \Phi^2 + [(\Phi^2 - 2\beta)(\Phi^2 - 2)]^{1/2}}. \tag{B5}$$

[1] J. Evans, Am. J. Phys. **61**, 347 (1993).
[2] C. Tzanakis, Eur. J. Phys. **19**, 69 (1998).
[3] J. D. Joannopoulos, R. D. Meade, and J. N. Winn, *Photonic Crystals* (Princeton University, Princeton, NJ, 1995).
[4] A. M. Steinberg, P. G. Kwiat, and R. Y. Chiao, Phys. Rev. Lett. **71**, 708 (1993).
[5] Ch. Spielmann, R. Szipöcs, A. Stingl, and F. Krausz, Phys. Rev. Lett. **73**, 2308 (1994).
[6] P. Balcou and L. Dutriaux, Phys. Rev. Lett. **78**, 851 (1997).
[7] S. Longhi, P. Laporta, M. Belmonte, and E. Recami, Phys. Rev. E **65**, 046610 (2002).
[8] L. Sirko, P. M. Koch, and R. Blumel, Phys. Rev. Lett. **78**, 2940 (1997).
[9] R. Morandotti, U. Peschel, J. S. Aitchison, H. S. Eisenberg, and Y. Silberberg, Phys. Rev. Lett. **83**, 4756 (1999).
[10] T. Pertsch, P. Dannberg, W. Elflein, A. Brauer, and F. Lederer, Phys. Rev. Lett. **83**, 4752 (1999).
[11] G. Lenz, I. Talanina, and C. M. de Sterke, Phys. Rev. Lett. **83**, 963 (1999).
[12] M. Rusek and A. Orlowski, Phys. Rev. E **59**, 3655 (1999).
[13] S. Longhi, Phys. Rev. E **65**, 027601 (2002).
[14] J. A. Sanchez-Gil and V. Freilikher, Phys. Rev. B **68**, 075103 (2003).
[15] S. Longhi, D. Janner, M. Marano, and P. Laporta, Phys. Rev. E **67**, 036601 (2003).
[16] J. A. Arnaud, J. Opt. Soc. Am. **65**, 174 (1975).
[17] W. K. Kahn and S. Yang, J. Opt. Soc. Am. **73**, 684 (1983).
[18] R. J. Black and A. Ankiewicz, Am. J. Phys. **53**, 554 (1985).
[19] A. K. Ghatak and E. Sauter, Eur. J. Phys. **10**, 136 (1989).
[20] E. Sauter and A. K. Ghatak, Eur. J. Phys. **10**, 144 (1989).
[21] N. Marinescu, Prog. Quantum Electron. **16**, 183 (1992).
[22] J. J. Garcia-Ripoll, V. M. Perez-Garcia, and P. Torres, Phys. Rev. Lett. **83**, 1715 (1999).
[23] V. M. Perez-Garcia, P. Torres, J. J. Garcia-Ripoll, and H. Michinel, J. Opt. B: Quantum Semiclassical Opt. **2**, 353 (2000).
[24] D. W. Berreman, Bell Syst. Tech. J. **45**, 2117 (1965); J. Hirano, and Y. Fukatsu, Proc. IEEE **52**, 1284 (1964); D. Marcuse, Bell Syst. Tech. J. **43**, 2065 (1965).
[25] R. A. Abram, Opt. Commun. **12**, 338 (1974).
[26] A. Hardy, Appl. Phys. **18**, 223 (1979).
[27] S. Longhi, Opt. Commun. **176**, 327 (2000).
[28] J. J. G. Ripoll and V. M. Perez-Garcia, Phys. Rev. A **59**, 2220 (1999).
[29] H. Lamb, *Dynamics*, 2nd ed. (Cambridge University Press, Cambridge, UK, 1923), Chap. IV, Sec. 33.
[30] S. Sinha and Y. Castin, Phys. Rev. Lett. **87**, 190402 (2001).
[31] A. Recati, F. Zambelli, and S. Stringari, Phys. Rev. Lett. **86**, 377 (2001).
[32] K. Kasamatsu, M. Tsubota, and M. Ueda, Phys. Rev. A **67**, 033610 (2003).
[33] E. Lundh, J.-P. Martikainen, and K.-A. Suominen, Phys. Rev. A **67**, 063604 (2003).
[34] D. Gloge and D. Marcuse, J. Opt. Soc. Am. **59**, 1629 (1969).
[35] J. A. Arnaud, *Beam and Fiber Optics* (Academic, New York, 1976), pp. 173–177.
[36] M. J. Adams, *An Introduction to Optical Waveguides* (Wiley, New York, 1981).
[37] R. Accornero, M. Artiglia, G. Coppa, P. di Vita, G. Lapenta, M. Potenza, and P. Ravetto, Electron. Lett. **26**, 1959 (1990).
[38] S. Takagi, Prog. Theor. Phys. **85**, 463 (1991).
[39] S. N. Vlasov, V. A. Petrischev, and V. I. Talanov, Radiophys. Quantum Electron. **14**, 1062 (1971); P. A. Belanger, Opt. Lett. **16**, 196 (1991); M. A. Porras, J. Alda, and E. Bernabeu, Appl. Opt. **32**, 5885 (1993).
[40] I. Bialynicki-Birula and Z. Bialynicka-Birula, Phys. Rev. A **65**, 063606 (2002).